HHS Public Access

Author manuscript

Sci Transl Med. Author manuscript; available in PMC 2017 June 20.

Published in final edited form as:

Sci Transl Med. 2016 July 27; 8(349): 349ra99. doi:10.1126/scitranslmed.aaf3838.

Curative ex vivo liver-directed gene therapy in a pig model of hereditary tyrosinemia type 1

Raymond D. Hickey[1,2,*], **Shennen A. Mao**[1], **Jaime Glorioso**[1], **Faysal Elgilani**[1], **Bruce Amiot**[3], **Harvey Chen**[1], **Piero Rinaldo**[4], **Ronald Marler**[5], **Huailei Jiang**[6], **Timothy R. DeGrado**[6], **Lukkana Suksanpaisan**[6,7], **Michael K. O'Connor**[6], **Brittany L. Freeman**[8], **Samar H. Ibrahim**[8], **Kah Whye Peng**[2], **Cary O. Harding**[9], **Chak-Sum Ho**[10], **Markus Grompe**[11], **Yasuhiro Ikeda**[2], **Joseph B. Lillegard**[1,12], **Stephen J. Russell**[2], and **Scott L. Nyberg**[1]

[1]Department of Surgery, Mayo Clinic, Rochester, MN 55905, USA

[2]Department of Molecular Medicine, Mayo Clinic, Rochester, MN 55905, USA

[3]Brami Biomedical Inc., Coon Rapids, MN 55433, USA

[4]Division of Laboratory Genetics, Department of Laboratory Medicine and Pathology, Mayo Clinic, Rochester, MN 55905, USA

[5]Department of Comparative Medicine, Mayo Clinic, Scottsdale, AZ 85259, USA

[6]Department of Radiology, Mayo Clinic, Rochester, MN 55905, USA

[7]Imanis Life Sciences, Rochester, MN 55902, USA

[8]Division of Pediatric Gastroenterology, Mayo Clinic, Rochester, MN 55905, USA

[9]Department of Molecular and Medical Genetics and Department of Pediatrics, Oregon Health and Science University, Portland, OR 97239, USA

[10]Histocompatibility Laboratory, Gift of Life Michigan, Ann Arbor, MI 48108, USA

[11]Papé Family Pediatric Research Institute, Oregon Health and Science University, Portland, OR 97239, USA

[12]Midwest Fetal Care Center, Children's Hospitals and Clinics of Minnesota, Minneapolis, MN 55404, USA

Abstract

We tested the hypothesis that ex vivo hepatocyte gene therapy can correct the metabolic disorder in fumarylacetoacetate hydrolase–deficient (*Fah*$^{-/-}$) pigs, a large animal model of hereditary

*Corresponding author. hickey.raymond@mayo.edu.

Author contributions: R.D.H., S.A.M., J.G., F.E., and S.L.N. designed experiments, performed experiments, interpreted results, and wrote the paper. B.A. performed hepatocyte isolations. H.C. provided surgical expertise. P.R. and C.O.H. facilitated biochemical data collection and analysis. R.M. provided pathology reports. H.J. and T.R.D. provided radioisotope for PET/CT imaging. L.S. and M.K.O. analyzed PET/CT data. B.L.F. and S.H.I. performed TUNEL assay and analysis. C.-S.H. conducted the SLA typing and interpretation. K.W.P., M.G., Y.I., J.B.L., and S.J.R. provided intellectual input, designed experiments, and interpreted data.

Competing interests: The authors declare that they have no competing interests.

Data and materials availability: All data are shown, and all materials are commercially available or are available from the corresponding author upon request.

tyrosinemia type 1 (HT1). Recipient *Fah*$^{-/-}$pigs underwent partial liver resection and hepatocyte isolation by collagenase digestion. Hepatocytes were transduced with one or both of the lentiviral vectors expressing the therapeutic *Fah* and the reporter sodium-iodide sym-porter (*Nis*) genes under control of the thyroxine-binding globulin promoter. Pigs received autologous transplants of hepatocytes by portal vein infusion. After transplantation, the protective drug 2-(2-nitro-4-trifluoromethylbenzyol)-1,3 cyclohexanedione (NTBC) was withheld from recipient pigs to provide a selective advantage for expansion of corrected FAH^{+} cells. Proliferation of transplanted cells, assessed by both immunohistochemistry and noninvasive positron emission tomography imaging of NIS-labeled cells, demonstrated near-complete liver repopulation by gene-corrected cells. Tyrosine and succinylacetone levels improved to within normal range, demonstrating complete correction of tyrosine metabolism. In addition, repopulation of the *Fah*$^{-/-}$ liver with transplanted cells inhibited the onset of severe fibrosis, a characteristic of nontransplanted *Fah*$^{-/-}$ pigs. This study demonstrates correction of disease in a pig model of metabolic liver disease by ex vivo gene therapy. To date, ex vivo gene therapy has only been successful in small animal models. We conclude that further exploration of ex vivo hepatocyte genetic correction is warranted for clinical use.

INTRODUCTION

Hereditary tyrosinemia type 1 (HT1) is an autosomal recessive inborn error of metabolism, caused by deficiency in fumarylacetoacetate hydrolase (FAH), an enzyme that catalyzes the last step of tyrosine metabolism (1, 2). Absence of FAH causes accumulation of fumarylacetoacetate, resulting in mutagenic, cytostatic, and acutely apoptotic events within the cell (3–5). Acute onset of HT1 is characterized by severe liver dysfunction (6), most frequently leading to death, if untreated. The chronic form of HT1 is characterized by progressive liver disease, typically severe fibrosis and hepatocellular carcinoma. The most common treatment for HT1 is a low-tyrosine diet combined with administration of 2-(2-nitro-4-trifluoromethylbenzyol)-1,3 cyclohexanedione (NTBC) (7), a potent inhibitor of 4-hydroxyphenylpyruvate dioxygenase, an enzyme in the tyrosine metabolic pathway. However, some patients are refractory to NTBC therapy, and those on NTBC remain at increased risk of several conditions, including cirrhosis, hepatocellular carcinoma, and impaired intellectual development (8). Therefore, liver transplantation remains the only curative therapy for this disease.

We have recently demonstrated that transplantation of wild-type syngeneic hepatocytes can correct metabolic disease in FAH-deficient (*Fah*$^{-/-}$) mice, a model of HT1 (9). We were able to show that regenerating hepatocytes in this mouse model can be noninvasively imaged using the sodium-iodide symporter (*Nis*) gene to label the cells. NIS-positive cells can take up radiolabeled iodine, or its analogs, and therefore be imaged using single-photon emission computed tomography (SPECT) or positron emission tomography (PET). This study in rodents therefore corroborated previous data demonstrating the potential efficacy of hepatocyte transplantation in treating metabolic liver diseases (10, 11). To further test the efficacy of cell transplantation in a clinically relevant setting, we looked toward a large animal model of HT1: the previously generated and characterized *Fah*$^{-/-}$ pig (12, 13). In the absence of NTBC, *Fah*$^{-/-}$ pigs undergo acute liver failure that is characterized by diffuse and

severe hepatocellular damage (12). When *Fah*$^{-/-}$ pigs are cycled on and off low-dose NTBC, animals undergo progressive clinical decline that results in chronic liver failure and severe fibrosis (14). *Fah*$^{-/-}$ pigs therefore provide a unique genetically engineered large animal model of a metabolic disease to test regenerative therapies, such as ex vivo gene therapy.

After some successful ex vivo gene therapy interventions in small animal models of liver disease, including a rabbit model of familial hypercholesterolemia (15), a single clinical trial of ex vivo gene therapy was undertaken nearly two decades ago using a gammaretroviral vector to treat five patients with familial hypercholesterolemia by modifying autologous primary hepatocytes (16). Although a modest therapeutic benefit was observed in some of the patients, this approach was limited by poor transduction efficiencies using gammaretroviruses and limited engraftment of corrected cells. As a result, no further clinical trials using ex vivo gene therapy for liver disease have occurred. More recently, however, the success of ex vivo gene therapy in hematopoietic stem cells for treating hematological disorders using lentiviral vectors (LV) (17, 18) raises the possibility that similar success can be achieved in treating metabolic liver diseases. LVs have a number of key advantages for hepatocyte gene therapy, including the ability to infect nondividing cells, sustained gene delivery through integration, and safer integration site profiles than those of gammaretroviruses (19). The efficacy of such an approach has been demonstrated in a small animal model of HT1 (20). Here, we demonstrate that ex vivo gene therapy in autologous hepatocytes can prevent liver failure and correct metabolic function in *Fah*$^{-/-}$ pigs, setting the stage for translation of this approach to human metabolic liver diseases.

RESULTS

Allogeneic hepatocyte transplantation cannot correct metabolic disease in *Fah*$^{-/-}$ pigs

To date, the vast majority of human hepatocyte transplantations for metabolic liver diseases have been of allogeneic source (21, 22). To simulate clinical human hepatocyte transplantation, we tested the efficacy of allogeneic hepatocyte transplant in *Fah*$^{-/-}$ pigs. We first characterized the genetic loci governing the pig swine leukocyte antigen (*Sla*) and *Fah* genes (23, 24). The *Sla* gene complex is located on *Sus scrofa* chromosome 7 (SSC7), with class I on the short (p) arm and class II on the long (q) arm, spanning the centromere. Our data predicted that *Fah* is located on the long arm of SSC7, telomeric to the *Sla* class II region, about 27 million base pairs from the major histocompatibility complex class II antigen *Sla-Drb1* gene (fig. S1A).

On the basis of SLA typing results (fig. S1B), we performed a transplant of *Sla*-matched allogeneic FAH^{+} hepatocytes from a heterozygote *Fah*$^{+/-}$ pig (Y501) into a single *Fah*$^{-/-}$ pig (Y502) (table S1). Isolated hepatocytes were injected through the portal vein, and NTBC was periodically removed from the diet to stimulate expansion of transplanted FAH^{+} cells. The animal did not show clinical improvement nor did it become NTBC-independent (fig. S1C). Histological analysis demonstrated the absence of any transplanted FAH^{+} cells (fig. S1D). On the basis of these results, we focused the remaining experiments on using gene therapy in autologous hepatocytes.

Ex vivo hepatocyte gene therapy corrects HT1 in mice

A vesicular stomatitis virus glycoprotein G–pseudotyped LV was produced that expressed the porcine *Fah* cDNA under the control of a liver-specific promoter containing the human thyroxine-binding globulin (TBG) promoter and two copies of the α1-microglobulin/bikunin enhancer (referred to as TBG throughout) (Fig. 1A) (25). To test the efficacy of this vector in vivo, we first transplanted donor $Fah^{-/-}$ mouse hepatocytes that were transduced with LV-*Fah* into syngeneic $Fah^{-/-}$ mice by intrasplenic injection (Fig. 1B). NTBC was withheld periodically (mice were on NTBC from days 15 to 20 and 43 to 48 after transplant) to allow expansion of transplanted cells (26). Two mice were euthanized, and the livers were harvested at three time points: days 14, 40, and 148 after transplantation (Fig. 1B). All recipient $Fah^{-/-}$ mice showed engraftment of LV-transduced hepatocytes, and there was substantial, albeit non-homogeneous, expansion of the cells at the two later time points, indicating differences in initial engraftment of cells between lobes (Fig. 1, C and D). In mouse livers harvested at day 148, there was almost complete repopulation of the host tissue by LV-transduced hepatocytes. Liver cell repopulation corresponded with normalization of biochemical indicators of liver function in $Fah^{-/-}$ mice, whereas mice receiving no cell transplants had severely impaired liver function and disease (Fig. 1E).

Ex vivo hepatocyte gene therapy was tested in four $Fah^{-/-}$ pigs

On the basis of promising results in mouse models of HT1, we proceeded to testing ex vivo gene therapy in the pig model of HT1 (Fig. 2A). Our group had previously demonstrated the benefit of dexamethasone in increasing LV transduction in mouse hepatocytes ex vivo (9). Using this protocol, ~80% of primary pig hepatocytes were transduced with an LV at a multiplicity of infection (MOI) of 2000 physical lentiviral particles (LPs), and ~60% of cells were transduced at an MOI of 500 LPs (Fig. 2B).

A total of four $Fah^{-/-}$ pigs underwent ex vivo gene therapy for this study (table S1 and Fig. 2A). Animals underwent a partial liver resection by midline laparotomy. About 10% of the liver was removed and hepatocytes were isolated, with cell viability after purification ranging from 88 to 92%. Hepatocytes were transduced with one or both of LV-*Fah* and LV-*Nis* (to use to track the cells noninvasively) in suspension. FAH expression was confirmed in transduced hepatocytes from all four donors (Fig. 2C). Viability and plateability of hepatocytes were confirmed after LV transduction, and no differences were observed between control and transduced cells (Fig. 2D). After LV transduction, between 350 and 864 million live cells were injected through the portal vein, either by direct catheterization of the portal vein or using ultrasound guidance to inject hepatocytes percutaneously (fig. S2 and movie S1). No adverse events were encountered with the surgery, and all animals were ambulatory and feeding within 24 hours.

LV-transduced hepatocytes engraft and proliferate in vivo in pigs

All animals remained on NTBC for 48hoursaftersurgery(Fig. 2A). At this point, NTBC was removed from the diet to stimulate expansion of transplanted cells. Animals were cycled on and off NTBC until weight stabilization occurred. From this point on, animals did not receive NTBC. Two animals (Y707 and Y846) were euthanized early in the study to test the efficacy of the ex vivo gene therapy approach in pigs and to determine whether a selective

advantage for FAH^+ cells exists in this model. Both animals appeared to achieve weight stability off NTBC (Fig. 3A), indicating that expansion of transplanted cells had occurred. In contrast to a nontransplanted *Fah*$^{-/-}$ pig (L768), robust FAH expression was detected in Y707 and Y846 at time of euthanasia (Fig. 3B). Individual clusters of FAH^+ cells were evident within the lobules of the pig parenchyma, consistent with expansion of single engrafted cells (Fig. 3C). Masson's trichrome staining revealed no evidence of severe fibrosis in either animal, and no major pathology was observed by hematoxylin and eosin (H&E) staining (Fig. 3B). On the basis of these results, we elected to determine the long-term effect of ex vivo gene therapy in the pig model of HT1.

Ex vivo hepatocyte gene therapy corrects metabolic deficiency in *Fah*$^{-/-}$ pigs

Pigs Y842 and Y845 were studied for 12 months, with one animal euthanized at this time point. The pigs exhibited NTBC-related weight fluctuations previously noted in *Fah*$^{-/-}$ mice (27). Both animals became completely independent of NTBC 95 days (Y842) and 140 days (Y845) after ex vivo gene therapy and hepatocyte transplantation (Fig. 4A). Consistent with NTBC-independence, these two pigs gained weight and did not manifest any failure-to-thrive phenotype that was previously noted in control *Fah*$^{-/-}$ pigs off NTBC (12).

Biochemical analysis was performed at 12 months. Reference values for wild-type and *Fah*$^{-/-}$ pigs off NTBC (*Fah*$^{-/-}$) were compiled from previous studies (12). *Fah*$^{-/-}$ pigs receiving LV-*Fah* had normal liver function that was characterized by markedly reduced plasma levels of total bilirubin and ammonia, compared to *Fah*$^{-/-}$ pigs off NTBC (12) (Fig. 4B). Comparable to wild-type animals (12), *Fah*$^{-/-}$pigs that underwent ex vivo gene therapy had considerably reduced levels of both tyrosine and succinylacetone, which are diagnostic for HT1 in humans and pigs (Fig. 4B). Additionally, plasma concentrations of methionine were reduced in animals Y842 and Y845.

LV-*Fah*–transduced hepatocytes completely repopulate *Fah*$^{-/-}$ pig livers

To determine the degree of repopulation of LV-*Fah*–transduced hepatocytes, pig Y845 was euthanized at 12 months after transplantation, and FAH IHC was performed. FAH staining revealed near-complete repopulation of the recipient liver by FAH^+ cells (Fig. 5A). Individual lobules appeared to be engrafted by one to two FAH^+ hepatocytes that subsequently proliferated extensively to repopulate the entire lobule. Individual hepatocyte clones were uniquely identified by variations in FAH-staining intensity between and within lobules (Fig. 5A).

We next determined the average number of LV integrations in the repopulated liver tissue from Y842 and Y845 using quantitative polymerase chain reaction (qPCR). On the basis of this analysis, we calculated an average of 0.13 copies of the LV vector per haploid genome (Fig. 5B). Given the ploidy content of hepatocytes and the proportion of hepatocytes in the liver, this integration frequency indicates an average of one LV integration per hepatocyte, consistent with the in vitro transduction frequencies (Fig. 2B). Last, the proportion of cells undergoing proliferation and apoptosis was determined in livers from all pigs using Ki67 and terminal deoxynucleotidyl transferase–mediated deoxyuridine triphosphate nick end labeling (TUNEL) staining, respectively. All transplanted livers had increased numbers of

proliferating cells compared to control pigs, consistent with FAH^+ cells repopulating the $Fah^{-/-}$ liver (Fig. 5C and fig. S3). No significant increase in apoptosis was detected in transplanted livers compared to controls (Fig. 5D and fig. S3).

NIS-labeled hepatocytes can be imaged noninvasively in vivo

Eight months after hepatocyte transplantation in pig Y842, we performed noninvasive imaging of repopulating cells using PET/CT imaging with the iodide analog [^{18}F]tetrafluoroborate ([^{18}F]TFB). In this animal, autologous hepatocytes were transduced with both LV-*Fah* and LV-*Nis* (table S1). On the basis of studies with GFP and red fluorescent protein (RFP), we estimate that 50 to 60% of cells were doubly FAH^+NIS^+ (Fig. 6A). Because cells in the liver do not express *Nis* (9), only LV-*Nis*–transduced hepatocytes should take up iodine and be detected by PET imaging with [^{18}F]TFB. The ability of LV-*Nis*–transduced hepatocytes to take up radiolabeled iodide (^{125}I) intracellularly was confirmed initially in vitro (Fig. 6B).

In vivo, in a control wild-type pig, uptake of [^{18}F]TFB was detected only in the stomach and not in the liver (Fig. 6C), consistent with data from mouse studies (28). In contrast, pig Y842 demonstrated significant uptake of [^{18}F]TFB in the liver, thus allowing noninvasive evaluation of repopulating clusters of FAH^+ cells (Fig. 6C). These PET/CT data were validated by laparoscopic biopsies demonstrating robust expansion of the LV-*Fah*–transduced hepatocytes in the liver of Y842 (Fig. 5A).

Repopulation by FAH^+ cells prevents onset of severe fibrosis

Although livers from pigs Y707 (analyzed 2 months after transplant) and Y846 (analyzed 4 months after transplant) demonstrated periportal or lobular fibrous connective tissue within normal limits (Fig. 3B), the long-term effect of ex vivo gene therapy on the onset of fibrosis was unknown. $Fah^{-/-}$ pigs maintained on very low doses of NTBC exhibit significant increases in fibrosis and portal hypertension (14). In contrast, in both pigs that received *FAH*-corrected hepatocyte transplants, repopulation of the $Fah^{-/-}$ liver prevented the progression of severe fibrosis (Fig. 7). In these two pigs, there was a significant decrease in fibrosis, as quantified by Masson's trichrome staining, compared to $Fah^{-/-}$ pigs cycled on and off NTBC (Fig. 7).

Variation in staining using Masson's trichrome did exist between different lobes in Y845 (fig. S4), in which the severity grade for fibrosis was scored by the pathologist from minimal (majority of the liver) to moderate (minority of the liver) fibrosis. Variations in the degree of fibrosis appeared to be associated with differences in cell engraftment in different lobes, a characteristic that was also noted between lobes in the mouse experiments (Fig. 1D). In addition, histopathological analysis of liver tissue revealed no evidence of hepatocellular carcinoma (Figs. 3 and 7)—an important consideration given the potential risk of insertional mutagenesis that has been reported by ex vivo gene therapy approaches with gammaretroviral vectors for treating some primary immunodeficiency diseases (29).

DISCUSSION

Although the individual incidence of each inborn error of metabolism disorder is rare, it is estimated that 22% of all pediatric liver transplants resulted from metabolic disease (30). As the shortage of donor organs continues to limit organ transplantation, other therapeutic strategies are urgently required to treat this patient population with debilitating diseases. One potential alternative is hepatocyte transplantation. The results presented here from a large animal model of liver failure demonstrate that ex vivo gene therapy is indeed a potential alternative therapeutic strategy to whole-organ transplantation. Similar to the mouse model (26) and as has been reported in human HT1 patients (31), FAH^+ cells had the proliferative advantage to expand and repopulate the $Fah^{-/-}$ pig liver under selective NTBC withdrawal. Repopulation of the liver with FAH^+ cells produced a marked clinical outcome in which amelioration of the HT1 phenotype and prevention of fibrosis were achieved—a compelling finding for HT1 patients who experience severe fibrosis.

Several small-animal models of metabolic liver diseases have been treated successfully by hepatocyte transplantation (10, 11), paving the way for human hepatocyte transplantations to occur (22). However, nearly all human hepatocyte transplantations to date have involved allogeneic cells. Therefore, in addition to the need for long-term immunosuppression in the patient, results to date suggest that an immune response is still mounted against the transplanted allogeneic cells, causing loss of engrafted cells (32, 33). Successful application of ex vivo gene therapy in small animal models paved the way for an autologous ex vivo cell therapy approach to treat five patients with familial hypercholesteremia (16). In recent years, the advent of self-inactivating LV has resulted in the safe and efficacious treatment of several primary immunodeficiencies using ex vivo gene therapy (17, 18). Here, we confirmed that such an approach could be used to treat metabolic liver disorders. A major restraint of current transplantation techniques is the inability to monitor cells noninvasively and longitudinally after injection, particularly given the ability of hepatocytes to engraft and expand outside of the liver (34). We previously demonstrated noninvasive three-dimensional imaging of regenerating tissue in individual animals over time using NIS as a reporter gene in mouse hepatocytes (9). Here, we used PET/CT imaging combined with the iodide analog [^{18}F]TFB to detect FAH^+ hepatocytes noninvasively in one pig. Our imaging analysis, in combination with liver staining, showed expansion of individual FAH^+ hepatocytes throughout the parenchyma. Although imaging was only performed in one animal, the result validates NIS as a suitable noninvasive reporter for future cell transplantation studies.

There are some limitations to this study. First, although the results of these studies demonstrate the efficacy of an ex vivo gene therapy approach, we used only four experimental animals; only two were for the same amount of time. These data need to be reproduced in a larger cohort of animals because pigs, similar to humans—and unlike rodents—are outbred, and phenotypic differences do exist between different animals. Second, in future studies, there is a need to perform more rigorous testing of the insertion site profile of the LV (20). Although this was not yet possible given the current incomplete annotation status of the pig genome, it would be interesting to compare the insertion profile in pig cells to those of mouse and human hepatocytes, to determine whether any evidence of clonal selection occurs in this model. There are several challenges that will need to be

overcome before achieving successful clinical translation for metabolic diseases, in which a selective advantage does not exist for the corrected cell to proliferate. The two principal limitations are cell engraftment and proliferation. Although many protocols have been developed to attempt to overcome these barriers in small and large animals, including preparative irradiation and portal embolization (35–37), these protocols have yet to be applied to a suitable preclinical model of metabolic disease. It is our opinion that large animal models, such as the *Fah*$^{-/-}$ pigs used in this study, the dog model of hemophilia B, and the pig model of familial hypercholesterolemia (38, 39), should be used to a greater degree in preclinical translational work to accelerate clinical translation of novel regenerative therapies, including cell transplantation.

For clinical translation, we hypothesize that pediatric patients with inborn errors of metabolism of the liver are most likely to benefit from the significant advantages of ex vivo LV gene therapy when compared to other approaches being examined today. In contrast to AAV-mediated gene therapy, LV integration provides stable gene expression that is optimal for the treatment of pediatric patients in whom hepatocytes are actively dividing and growing. Furthermore, the recent clinical success in treating several primary immunodeficiency disorders using ex vivo gene therapy in hematopoietic cells sets a precedent for the use of LV-mediated gene therapy in children (17, 18). However, despite the clear demonstration of safety to date of LV in the clinic for primary immunodeficiencies, further work to test genotoxicity of LV in human hepatocytes is required before initiation of any clinical trials, particularly given the recent data on genotoxicity of other viral vectors, including AAV, in inducing hepatocellular carcinoma in rodent models (40). Once this has been demonstrated, we believe that ex vivo hepatocyte gene therapy with LV will provide a lasting impact for the treatment of inborn errors of metabolism of the liver in children before their disease has a chance to reach an advanced state.

MATERIALS AND METHODS

Study design

Our study was designed to test the hypothesis that ex vivo gene therapy in primary hepatocytes could correct and ameliorate disease in a large animal model of metabolic liver disease. We chose to use a pig model of HT1 for this purpose for clinical relevance. As a preliminary proof of concept, we used the mouse model of HT1 to test the efficacy of the LV expressing *Fah* to correct disease. Mice were randomly assigned to each experimental group. For the primary study, we used four pigs. Biochemical and histopathology data for wild-type and *Fah*$^{-/-}$ pigs off NTBC were compiled from previous studies (12). The use of historical controls and the low number of animals used were determined by the availability of this model and the need to comply with the regulations of the Institutional Animal Care and Use Committee at Mayo Clinic to limit the number of experimental animals. Investigators involved in histopathological and biochemical analyses were blinded. Investigators performing animal handling, sampling, euthanasia, and raw data collection were not blinded.

Animals and animal care

All animals received humane care in compliance with the regulations of the Institutional Animal Care and Use Committee at Mayo Clinic. *Fah*$^{-/-}$ mice (41) on the C57Bl/6J background were administered NTBC (Yecuris) in the drinking water at 8 mg/liter to prevent acute liver injury before transplantation. *Fah*$^{-/-}$ pigs were produced in a 50% Large White and 50% Landrace pig (12, 13). NTBC was administered to the animals orally, mixed within a portion of daily chow rations. Pregnant sows were given 25 to 50 mg of NTBC per day for the duration of gestation. Initial testing of dose and efficacy determined that there was no difference between 25 and 50 mg per day; as a result, two pregnant animals received 50 mg of NTBC per day, whereas the later pigs received only 25 mg per day. Weaned piglets were administered NTBC (1 mg/kg) per day until hepatocyte transplantation. All animals were observed at least daily for clinical signs and symptoms consistent with HT1 and acute liver failure. All animals were weighed daily for the first month, twice weekly up to 3 months, and then weekly until the end of the study. Control animals, including wild-type and *Fah*$^{-/-}$ pigs, have been described previously (12, 14).

Hepatocyte isolation, transduction, and transplantation

All animals undergoing cell transplantation received a femoral arterial line placement to monitor blood pressure. In addition, body temperature, respiration rate, and heart rate were continually monitored and recorded. For ex vivo gene therapy, after a midline laparotomy, pigs underwent a segmental liver resection using a Cavitron Ultrasonic Surgical Aspirator to complete the parenchymal transection. About 10% of the liver was removed. The liver specimen underwent an ex vivo two-step perfusion, and hepatocytes were isolated as described previously (42). Hepatocytes were transduced in suspension for 2 to 16 hours at the MOI indicated in table S1. Hepatocyte medium was identical to that described previously (9), which included 10 μM dexamethasone (Sigma-Aldrich). After two centrifugation washes, hepatocytes were resuspended in saline at a concentration of 10×10^6 to 20×10^6 cells/ml and transplanted through a portal vein infusion. For percutaneous injection, the portal vein was identified by surface ultrasound using a 2- to 5-MHz transducer (SonoSite). Under ultrasound guidance, an 18-gauge needle was directed percutaneously into the portal vein for injection of hepatocytes (movie S1). For transplantation of allogeneic cells in pig Y502, hepatocytes were isolated and transplanted as above, except that no transduction with LV occurred. After transplantation, all animals received continuous monitoring of vital signs until they recovered from anesthesia and became fully ambulatory. For the sham control pig L768 who received no cells, no surgery was performed, and the animal was cycled on and off NTBC.

Mouse experiments were performed as described previously (9). Briefly, hepatocytes were harvested from *Fah*$^{-/-}$ donor mice using a standard two-step collagenase digestion and centrifugal purification. Hepatocytes were cultured for 24 hours in six-well Primaria culture plates (BD Biosciences) during which LV-*Fah* was added at an MOI of 2000 LPs. Hepatocytes were trypsinized, and 0.5×10^6 cells were injected through the spleen into syngeneic *Fah*$^{-/-}$ mice.

PET imaging and analysis

Imaging was performed on the high-resolution GE Discovery 690 ADC PET/CT system (GE Healthcare). [^{18}F]TFB was synthesized as described previously (43). A single injection of [^{18}F]TFB was infused intravenously 75 min before scanning (dose of ~11 mCi at time of injection). CT was performed at 120 kV and 150 mA, with tube rotation of 0.5 s and pitch of 0.516. PET was performed as a two-bed acquisition with 10 min per bed and 17 slice overlap, resulting in a 27-cm axial field of view. Coregistered images were rendered and visualized using the PMOD software (PMOD Technologies). Location of liver and spleen was determined from the CT image.

Histopathological analysis

For tissue analysis, samples were fixed in 10% neutral buffered formalin (PROTOCOL, Fisher Scientific) and processed for paraffin embedding and sectioning. For H&E staining and Masson's trichrome staining, slides were prepared using standard protocols. Quantification of fibrosis was performed on Masson's trichrome–stained slides by analysis of digital images using Aperio ImageScope software (version 12.1). Quantification of collagen positivity in 10 random areas measuring 2 mm^3 each was performed in each slide using the Positive Pixel Count algorithm that is altered with a hue value of 0.62, hue width of 0.40, and color saturation threshold of 0.005. IHC for FAH (44) and Ki67 (MIB-1; Dako) was performed with a BOND-III automatic stainer (Leica), with a 20-min antigen retrieval step using BOND Epitope Retrieval Solution 2 (Leica), and stained with diaminobenzidine (Leica). Quantification of Ki67$^+$ cells was performed using Aperio ImageScope software Nuclear algorithm (version 9) in10 random areas measuring 0.25 mm^3 each. Terminal TUNEL staining was performed as described previously (45) using the ApopTag Peroxidase In Situ Apoptosis Detection Kit (Millipore).

Quantitative analysis of vector integration

DNA was isolated from total liver using a DNeasy Blood and Tissue Kit (Qiagen). Primers (5′-CGAGATCTGAGTCCGGTAGC-3′ and 5′-CCGACCTCCCTAACCCTATG-3′) were designed to amplify integrated vectors in the pig genome. qPCR was performed with Bullseye EvaGreen qPCR MasterMix (MidSci) using an initial denaturation step at 95°C for 10 min, followed by 40 cycles at 95°C for 15 s and at 60°C for 60 s. Absolute copy number was determined using a standard curve ranging from 3.21×10^5 to 2.05×10^1 copies of the vector plasmid. All samples were run in triplicate using 150 ng of DNA.

Statistical analysis

Results are expressed as means ± SD or SEM, as stated in figure captions. Statistical analyses were conducted with GraphPad Prism software version 6. Experimental differences between two groups were evaluated by Student's two-tailed *t* test, assuming equal variance. For comparison of biochemical parameters between pigs, because of the lack of available animals required to perform a randomized study, differences between experimental animals were compared to historical controls using a two-sided, independent *t* test with 5% type 1 error rate. Differences between multiple groups were compared using one-way ANOVA

followed by Bonferroni's multiple comparisons test. $P < 0.05$ was considered statistically significant.

Supplementary Material

Refer to Web version on PubMed Central for supplementary material.

Acknowledgments

We thank Exemplar Genetics for management of the *Fah*$^{-/-}$ herd; I. Ivanov (Mayo Clinic, Rochester) for biochemical analyses; L. Gross and T. Blahnik (Mayo Clinic, Rochester) and J. Pattengill (Mayo Clinic, Arizona) for histology support; L. Linscheid, D. McConnell, and B. Kemp (Mayo Clinic, Rochester) for PET imaging support; P. Novotny (Mayo Clinic, Rochester) for statistical analyses; D. Meixner for assistance with portal vein injections; M. Curry for figure preparation; and G. Gores (Mayo Clinic, Rochester) for thoughtful discussion.

Funding: R.D.H. was funded through an NIH K01 DK106056 award, an American Liver Foundation Postdoctoral Fellowship Award, and a Mayo Clinic Center for Regenerative Medicine Career Development Award. S.L.N. was funded through an NIH R41 DK092105 award, the Wallace H. Coulter Foundation, Marriot Foundation, Darwin Deason Family Foundation, and Mayo Foundation. S.H.I. was funded through the Center for Clinical and Translational Science KL2 program KL2TR000136-09 and the Mayo Clinic Center for Cell Signaling in Gastroenterology, Pilot and Feasibility Award, program P30DK084567.

REFERENCES AND NOTES

1. Lindblad B, Lindstedt S, Steen G. On the enzymic defects in hereditary tyrosinemia. Proc Natl Acad Sci USA. 1977; 74:4641–4645. [PubMed: 270706]
2. Edwards SW, Knox WE. Homogentisate metabolism: The isomerization of maleylacetoacetate by an enzyme which requires glutathione. J Biol Chem. 1956; 220:79–91. [PubMed: 13319328]
3. Endo F, Sun MS. Tyrosinaemia type I and apoptosis of hepatocytes and renal tubular cells. J Inherit Metab Dis. 2002; 25:227–234. [PubMed: 12137232]
4. Kubo S, Sun M, Miyahara M, Umeyama K, Urakami K-i, Yamamoto T, Jakobs C, Matsuda I, Endo F. Hepatocyte injury in tyrosinemia type 1 is induced by fumarylacetoacetate and is inhibited by caspase inhibitors. Proc Natl Acad Sci USA. 1998; 95:9552–9557. [PubMed: 9689118]
5. Jorquera R, Tanguay RM. The mutagenicity of the tyrosine metabolite, fumarylacetoacetate, is enhanced by glutathione depletion. Biochem Biophys Res Commun. 1997; 232:42–48. [PubMed: 9125148]
6. Russo P, O'Regan S. Visceral pathology of hereditary tyrosinemia type I. Am J Hum Genet. 1990; 47:317–324. [PubMed: 2378357]
7. Lindstedt S, Holme E, Lock EA, Hjalmarson O, Strandvik B. Treatment of hereditary tyrosinaemia type I by inhibition of 4-hydroxyphenylpyruvate dioxygenase. Lancet. 1992; 340:813–817. [PubMed: 1383656]
8. Mayorandan S, Meyer U, Gokcay G, Segarra NG, de Baulny HO, van Spronsen F, Zeman J, de Laet C, Spiekerkoetter U, Thimm E, Maiorana A, Dionisi-Vici C, Moeslinger D, Brunner-Krainz M, Lotz-Havla AS, Cocho de Juan JA, Couce Pico ML, Santer R, Scholl-Bürgi S, Mandel H, Bliksrud YT, Freisinger P, Aldamiz-Echevarria LJ, Hochuli M, Gautschi M, Endig J, Jordan J, McKiernan P, Ernst S, Morlot S, Vogel A, Sander J, Das AM. Cross-sectional study of 168 patients with hepatorenal tyrosinaemia and implications for clinical practice. Orphanet J Rare Dis. 2014; 9:107. [PubMed: 25081276]
9. Hickey RD, Mao SA, Amiot B, Suksanpaisan L, Miller A, Nace R, Glorioso J, O'Connor MK, Peng KW, Ikeda Y, Russell SJ, Nyberg SL. Noninvasive 3-dimensional imaging of liver regeneration in a mouse model of hereditary tyrosinemia type 1 using the sodium iodide symporter gene. Liver Transpl. 2015; 21:442–453. [PubMed: 25482651]
10. Matas AJ, Sutherland DE, Steffes MW, Mauer SM, Sowe A, Simmons RL, Najarian JS. Hepatocellular transplantation for metabolic deficiencies: Decrease of plasms bilirubin in Gunn rats. Science. 1976; 192:892–894. [PubMed: 818706]

11. Groth CG, Arborgh B, Björkén C, Sundberg B, Lundgren G. Correction of hyper-bilirubinemia in the glucuronyltransferase-deficient rat by intraportal hepatocyte transplantation. Transplant Proc. 1977; 9:313–316. [PubMed: 405772]
12. Hickey RD, Mao SA, Glorioso J, Lillegard JB, Fisher JE, Amiot B, Rinaldo P, Harding CO, Marler R, Finegold MJ, Grompe M, Nyberg SL. Fumarylacetoacetate hydrolase deficient pigs are a novel large animal model of metabolic liver disease. Stem Cell Res. 2014; 13:144–153. [PubMed: 24879068]
13. Hickey RD, Lillegard JB, Fisher JE, McKenzie TJ, Hofherr SE, Finegold MJ, Nyberg SL, Grompe M. Efficient production of *Fah*-null heterozygote pigs by chimeric adeno-associated virus-mediated gene knockout and somatic cell nuclear transfer. Hepatology. 2011; 54:1351–1359. [PubMed: 21674562]
14. Mao SA, Glorioso J, Hickey RD, Yin M, Lillegard J, Fisher JE, Marler RJ, Grompe M, Nyberg SL. A large animal model of portal hypertension and cirrhosis in the FAH-deficient pig. Hepatology. 2014; 60:1176a.
15. Chowdhury JR, Grossman M, Gupta S, Chowdhury NR, Baker JR Jr, Wilson JM. Long-term improvement of hypercholesterolemia after ex vivo gene therapy in LDLR-deficient rabbits. Science. 1991; 254:1802–1805. [PubMed: 1722351]
16. Grossman M, Rader DJ, Muller DWM, Kolansky DM, Kozarsky K, Clark BJ III, Stein EA, Lupien PJ, Brewer HB Jr, Raper SE, Wilson JM. A pilot study of ex vivo gene therapy for homozygous familial hypercholesterolaemia. Nat Med. 1995; 1:1148–1154. [PubMed: 7584986]
17. Aiuti A, Biasco L, Scaramuzza S, Ferrua F, Cicalese MP, Baricordi C, Dionisio F, Calabria A, Giannelli S, Castiello MC, Bosticardo M, Evangelio C, Assanelli A, Casiraghi M, Di Nunzio S, Callegaro L, Benati C, Rizzardi P, Pellin D, Di Serio C, Schmidt M, Von Kalle C, Gardner J, Mehta N, Neduva V, Dow DJ, Galy A, Miniero R, Finocchi A, Metin A, Banerjee PP, Orange JS, Galimberti S, Valsecchi MG, Biffi A, Montini E, Villa A, Ciceri F, Roncarolo MG, Naldini L. Lentiviral hematopoietic stem cell gene therapy in patients with Wiskott-Aldrich syndrome. Science. 2013; 341:1233151. [PubMed: 23845947]
18. Biffi A, Montini E, Lorioli L, Cesani M, Fumagalli F, Plati T, Baldoli C, Martino S, Calabria A, Canale S, Benedicenti F, Vallanti G, Biasco L, Leo S, Kabbara N, Zanetti G, Rizzo WB, Mehta NAL, Cicalese MP, Casiraghi M, Boelens JJ, Del Carro U, Dow DJ, Schmidt M, Assanelli A, Neduva V, Di Serio C, Stupka E, Gardner J, von Kalle C, Bordignon C, Ciceri F, Rovelli A, Roncarolo MG, Aiuti A, Sessa M, Naldini L. Lentiviral hematopoietic stem cell gene therapy benefits metachromatic leukodystrophy. Science. 2013; 341:1233158. [PubMed: 23845948]
19. Sakuma T, Barry MA, Ikeda Y. Lentiviral vectors: Basic to translational. Biochem J. 2012; 443:603–618. [PubMed: 22507128]
20. Rittelmeyer I, Rothe M, Brugman MH, Iken M, Schambach A, Manns MP, Baum C, Modlich U, Ott M. Hepatic lentiviral gene transfer is associated with clonal selection, but not with tumor formation in serially transplanted rodents. Hepatology. 2013; 58:397–408. [PubMed: 23258554]
21. Hughes RD, Mitry RR, Dhawan A. Current status of hepatocyte transplantation. Transplantation. 2012; 93:342–347. [PubMed: 22082820]
22. Jorns C, Ellis EC, Nowak G, Fischler B, Nemeth A, Strom SC, Ericzon BG. Hepatocyte transplantation for inherited metabolic diseases of the liver. J Intern Med. 2012; 272:201–223. [PubMed: 22789058]
23. Ho CS, Lunney JK, Franzo-Romain MH, Martens GW, Lee YJ, Lee JH, Wysocki M, Rowland RRR, Smith DM. Molecular characterization of swine leucocyte antigen class I genes in outbred pig populations. Anim Genet. 2009; 40:468–478. [PubMed: 19392823]
24. Ho CS, Lunney JK, Lee JH, Franzo-Romain MH, Martens GW, Rowland RRR, Smith DM. Molecular characterization of swine leucocyte antigen class II genes in outbred pig populations. Anim Genet. 2010; 41:428–432. [PubMed: 20121817]
25. Harding CO, Gillingham MB, Hamman K, Clark H, Goebel-Daghighi E, Bird A, Koeberl DD. Complete correction of hyperphenylalaninemia following liver-directed, recombinant AAV2/8 vector-mediated gene therapy in murine phenylketonuria. Gene Ther. 2006; 13:457–462. [PubMed: 16319949]

26. Overturf K, Al-Dhalimy M, Tanguay R, Brantly M, Ou CN, Finegold M, Grompe M. Hepatocytes corrected by gene therapy are selected in vivo in a murine model of hereditary tyrosinaemia type I. Nat Genet. 1996; 12:266–273. [PubMed: 8589717]
27. Overturf K, Al-Dhalimy M, Manning K, Ou CN, Finegold M, Grompe M. Ex vivo hepatic gene therapy of a mouse model of Hereditary Tyrosinemia Type I. Hum Gene Ther. 1998; 9:295–304. [PubMed: 9508047]
28. Jauregui-Osoro M, Sunassee K, Weeks AJ, Berry DJ, Paul RL, Cleij M, Banga JP, O'Doherty MJ, Marsden PK, Clarke SEM, Ballinger JR, Szanda I, Cheng SY, Blower PJ. Synthesis and biological evaluation of [^{18}F]tetrafluoroborate: A PET imaging agent for thyroid disease and reporter gene imaging of the sodium/iodide symporter. Eur J Nucl Med Mol Imaging. 2010; 37:2108–2116. [PubMed: 20577737]
29. Hacein-Bey-Abina S, Garrigue A, Wang GP, Soulier J, Lim A, Morillon E, Clappier E, Caccavelli L, Delabesse E, Beldjord K, Asnafi V, MacIntyre E, Dal Cortivo L, Radford I, Brousse N, Sigaux F, Moshous D, Hauer J, Borkhardt A, Belohradsky BH, Wintergerst U, Velez MC, Leiva L, Sorensen R, Wulffraat N, Blanche S, Bushman FD, Fischer A, Cavazzana-Calvo M. Insertional oncogenesis in 4 patients after retrovirus-mediated gene therapy of SCID-X1. J Clin Invest. 2008; 118:3132–3142. [PubMed: 18688285]
30. Hansen K, Horslen S. Metabolic liver disease in children. Liver Transpl. 2008; 14:713–733. [PubMed: 18433056]
31. Kvittingen EA, Rootwelt H, Brandtzaeg P, Bergan A, Berger R. Hereditary tyrosinemia type I. Self-induced correction of the fumarylacetoacetase defect. J Clin Invest. 1993; 91:1816–1821. [PubMed: 8473520]
32. Allen KJ, Mifsud NA, Williamson R, Bertolino P, Hardikar W. Cell-mediated rejection results in allograft loss after liver cell transplantation. Liver Transpl. 2008; 14:688–694. [PubMed: 18433045]
33. Han B, Lu Y, Meng B, Qu B. Cellular loss after allogenic hepatocyte transplantation. Transplantation. 2009; 87:1–5. [PubMed: 19136883]
34. Hoppo T, Komori J, Manohar R, Stolz DB, Lagasse E. Rescue of lethal hepatic failure by hepatized lymph nodes in mice. Gastroenterology. 2011; 140:656–666.e2. [PubMed: 21070777]
35. Koenig S, Yuan Q, Krause P, Christiansen H, Rave-Fraenk M, Kafert-Kasting S, Kriegbaum H, Schneider A, Ott M, Meyburg J. Regional transient portal ischemia and irradiation as preparative regimen for hepatocyte transplantation. Cell Transplant. 2011; 20:303–311. [PubMed: 20719089]
36. Zhou H, Dong X, Kabarriti R, Chen Y, Avsar Y, Wang X, Ding J, Liu L, Fox IJ, Roy-Chowdhury J, Roy-Chowdhury N, Guha C. Single liver lobe repopulation with wildtype hepatocytes using regional hepatic irradiation cures jaundice in Gunn rats. PLOS One. 2012; 7:e46775. [PubMed: 23091601]
37. Yamanouchi K, Zhou H, Roy-Chowdhury N, Macaluso F, Liu L, Yamamoto T, Yannam GR, Enke C, Solberg TD, Adelson AB, Platt JL, Fox IJ, Roy-Chowdhury J, Guha C. Hepatic irradiation augments engraftment of donor cells following hepatocyte transplantation. Hepatology. 2009; 49:258–267. [PubMed: 19003915]
38. Cantore A, Ranzani M, Bartholomae CC, Volpin M, Valle PD, Sanvito F, Sergi LS, Gallina P, Benedicenti F, Bellinger D, Raymer R, Merricks E, Bellintani F, Martin S, Doglioni C, D'Angelo A, VandenDriessche T, Chuah MK, Schmidt M, Nichols T, Montini E, Naldini L. Liver-directed lentiviral gene therapy in a dog model of hemophilia B. Sci Transl Med. 2015; 7:277ra228.
39. Davis BT, Wang XJ, Rohret JA, Struzynski JT, Merricks EP, Bellinger DA, Rohret FA, Nichols TC, Rogers CS. Targeted disruption of *LDLR* causes hypercholesterolemia and atherosclerosis in Yucatan miniature pigs. PLOS One. 2014; 9:e93457. [PubMed: 24691380]
40. Chandler RJ, LaFave MC, Varshney GK, Trivedi NS, Carrillo-Carrasco N, Senac JS, Wu W, Hoffmann V, Elkahloun AG, Burgess SM, Venditti CP. Vector design influences hepatic genotoxicity after adeno-associated virus gene therapy. J Clin Invest. 2015; 125:870–880. [PubMed: 25607839]
41. Grompe M, al-Dhalimy M, Finegold M, Ou C-N, Burlingame T, Kennaway NG, Soriano P. Loss of fumarylacetoacetate hydrolase is responsible for the neonatal hepatic dysfunction phenotype of lethal albino mice. Genes Dev. 1993; 7:2298–2307. [PubMed: 8253378]

42. Sielaff TD, Hu MY, Rao S, Groehler K, Olson D, Mann HJ, Remmel RP, Shatford RAD, Amiot B, Hu WS, Cerra FB. A technique for porcine hepatocyte harvest and description of differentiated metabolic functions in static culture. Transplantation. 1995; 59:1459–1463. [PubMed: 7770934]

43. Jiang H, Pandey MK, DeGrado TR. Synthesis of [18F]tetrafluoroborate via radiofluorination of BF3. J Labelled Compd Radiopharm. 2015; 58:S255.

44. Wang X, Montini E, Al-Dhalimy M, Lagasse E, Finegold M, Grompe M. Kinetics of liver repopulation after bone marrow transplantation. Am J Pathol. 2002; 161:565–574. [PubMed: 12163381]

45. Ibrahim SH, Gores GJ, Hirsova P, Kirby M, Miles L, Jaeschke A, Kohli R. Mixed lineage kinase 3 deficient mice are protected against the high fat high carbohydrate diet-induced steatohepatitis. Liver Int. 2014; 34:427–437. [PubMed: 24256559]

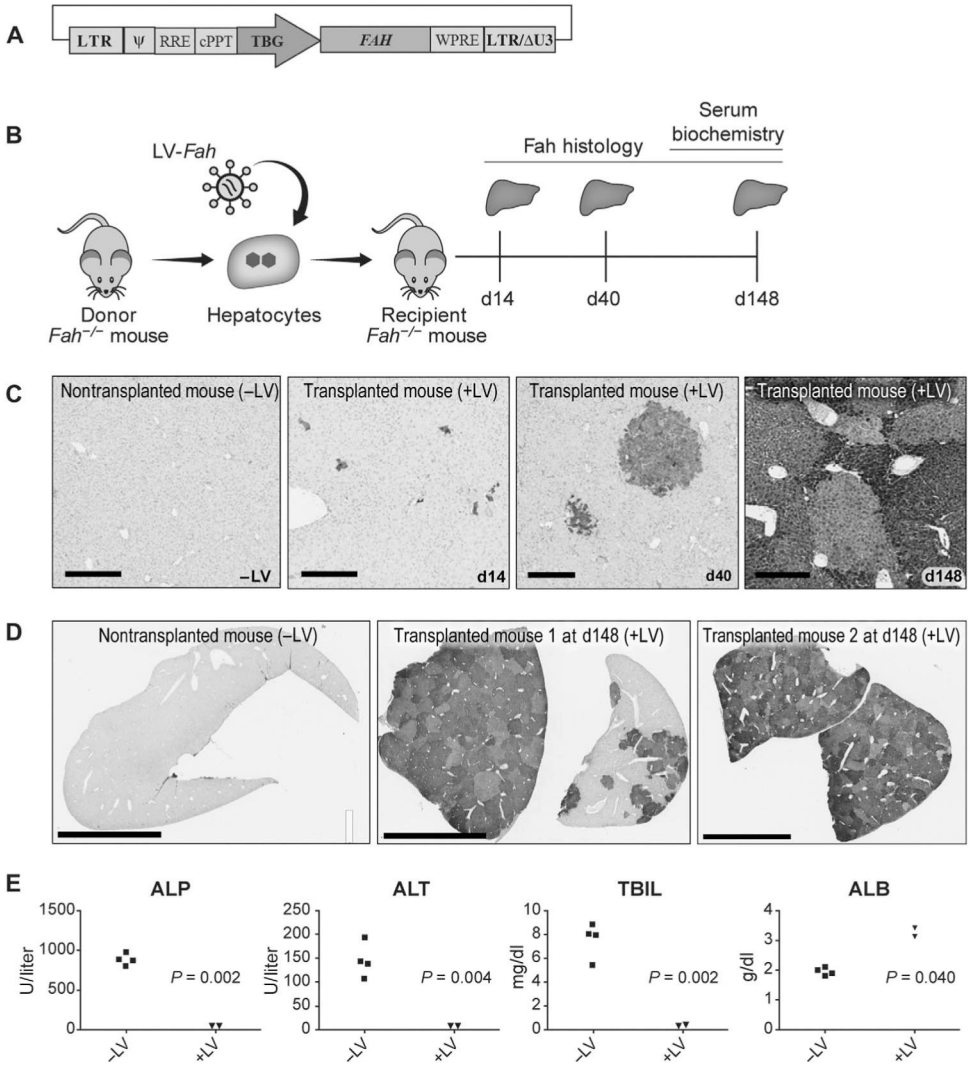

Fig. 1. Ex vivo gene therapy in *Fah*$^{-/-}$ mice using LV-*Fah* is curative

(**A**) Schematic representation of the LV used for mouse and pig studies in which the porcine *Fah* cDNA is under control of the human TBG promoter and two copies of a human α1-microglobulin/bikunin enhancer. LTR, long terminal repeat; Ψ, psi packaging sequence; RRE, Rev-responsive element; cPPT, central polypurine tract; WPRE, Woodchuck hepatitis virus posttranscriptional regulatory element; LTR/ΔU3, 3′ long terminal repeat with deletion in U3 region. (**B**) Mouse experiment timeline, where ex vivo transduced hepatocytes are transplanted into syngeneic recipient mice. Livers from recipients were collected at three time points: day 14 ($n = 2$), day 40 ($n = 2$), and day 148 ($n = 2$). d, day. (**C**) FAH immunohistochemistry (IHC) at days 14, 40, and 148 after transplantation. A nontransplanted mouse (−LV) is included as a negative control. Scale bars, 300 μm. (**D**) FAH IHC at lower magnification than (C) at day 148 after transplantation. A nontransplanted mouse (−LV) is included as a negative control. Scale bars, 4 mm. (**E**) Biochemical analysis of serum on day 148 comparing alkaline phosphatase (ALP), alanine aminotransferase (ALT), total bilirubin (TBIL), and albumin (ALB) in *Fah*$^{-/-}$ mice that underwent

transplantation with hepatocytes from *Fah*$^{-/-}$ mice that received no vector (−LV; $n = 4$) or were transduced ex vivo with LV-*Fah* (+LV; $n = 2$). Data are means ± SD. *P* values were determined using a two-tailed *t* test.

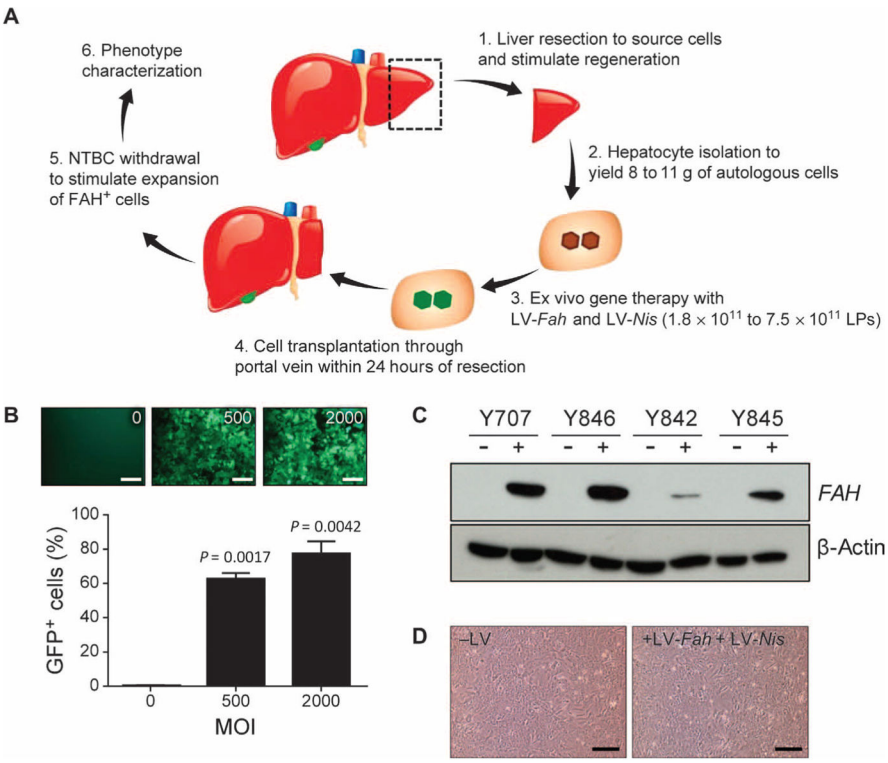

Fig. 2. Ex vivo gene therapy approach in *Fah*$^{-/-}$ pigs

(**A**) Schematic of the six steps involved in ex vivo gene therapy and liver repopulation in *Fah*$^{-/-}$ pigs: (1) partial hepatectomy was performed, and (2) hepatocytes were isolated by collagenase digestion. (3) Ex vivo gene therapy with an LV was performed before (4) retransplantation of the autologous cells. (5) NTBC was periodically withdrawn from the diet to stimulate expansion of the FAH^{+} cells. (6) Clinical evaluation, serum biochemistry analysis, and liver histopathological analysis were performed 2 (n = 1 pig), 4 (n = 1 pig), and 12 (n = 2 pigs) months after transplantation. (**B**) Percentage of green fluorescent protein (GFP)–positive hepatocytes detected by flow cytometry after transduction of cells with an LV expressing GFP at MOIs of 0, 500, and 2000 LPs. Flow cytometry was performed 72 hours after transduction. Data are means ± SD (n = 3 replicates). P values versus 0 MOI were determined using a two-tailed t test. Representative fluorescent images are also shown. Scale bars, 100 μm. (**C**) In vitro Western blot data confirming expression of FAH protein in pig hepatocytes after transduction ex vivo with LV-*Fah* (+) or untransduced cells (−) from the same animal. β-Actin served as loading control. (**D**) Representative images of plated hepatocytes from pig Y842 that were untransduced with LV (−LV) or were transduced with LV (+LV-*Fah* + LV-*Nis*). Scale bars, 100 μm.

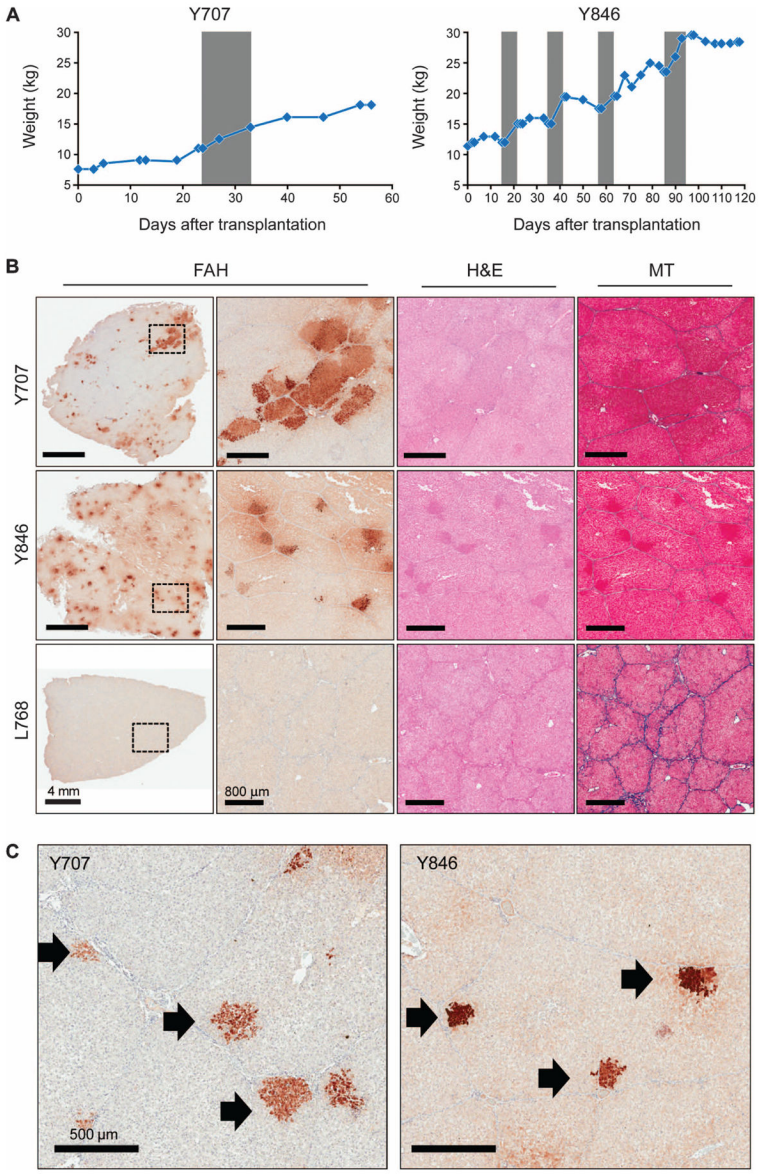

Fig. 3. LV-*Fah*–transduced hepatocytes proliferate extensively in vivo in pigs

Animals Y707 and Y846 were euthanized at 2 and 4 months after transplantation, respectively. Control $Fah^{-/-}$ pig L768 did not receive any gene-corrected hepatocytes but was cycled on and off NTBC. (**A**) Weight stabilization of pigs Y707 and Y846. Gray areas are times on NTBC (for Y707, from day 24 to day 32; for Y846, from days 14 to 21, 35 to 42, 57 to 64, and 86 to 93). (**B**) Representative liver tissues stained for FAH are shown at low and high magnification for each animal; the dotted rectangle indicates the area of enlargement. Serial sections of H&E–and Masson's trichrome (MT)–stained liver are also provided. Scale bars, 4 mm (low-magnification FAH); 800 μm (all other images). (**C**) FAH staining of liver tissue from pigs Y707 and Y846, identifying individual expanding hepatocyte nodules (black arrows).

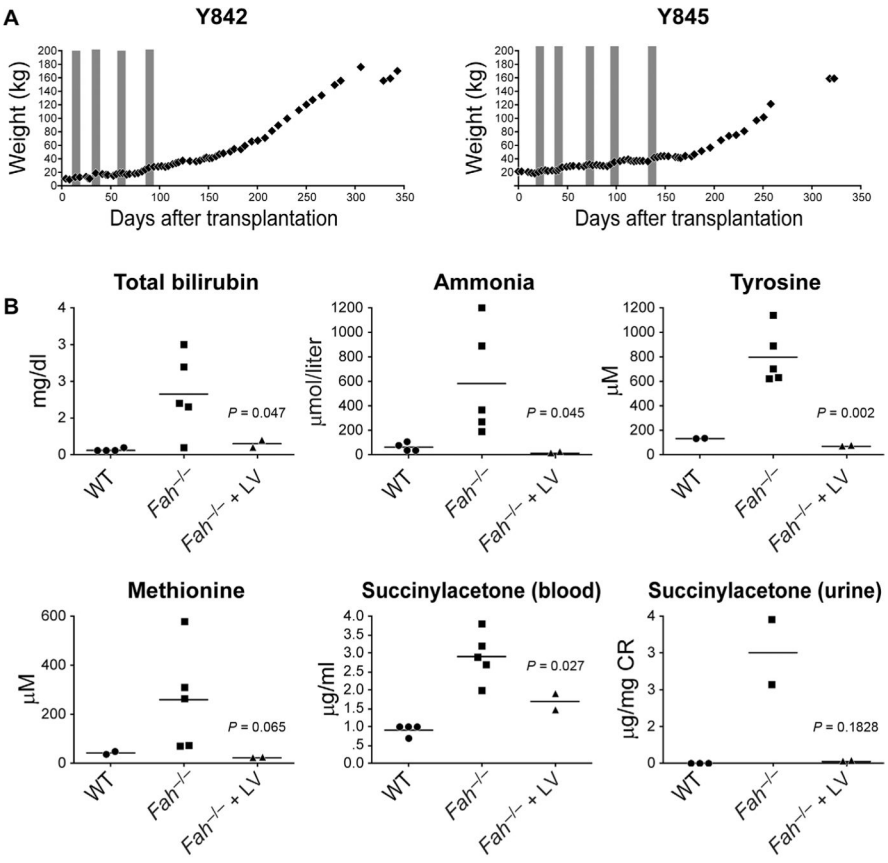

Fig. 4. Ex vivo hepatocyte gene therapy and transplantation in *Fah*$^{-/-}$ pigs corrects metabolic disease

(**A**) Weight charts of Y842 and Y845 in the proceeding days after transplantation. Time on NTBC is depicted in the gray shading (for Y842, from days 14 to 21, 34 to 41, 55 to 62, and 85 to 92; for Y845, from days 14 to 21, 37 to 44, 62 to 69, 94 to 101, and 131 to 138). (**B**) Plasma and serum biochemical analyses were performed at 12 months on pigs Y842 and Y845. Reference values for wild-type (WT) and *Fah*$^{-/-}$ pigs off NTBC (*Fah*$^{-/-}$) are compiled from previous studies (12). Individual data points for each animal are plotted with the mean of each group depicted with a line. *P* values were determined using a two-sided independent *t* test.

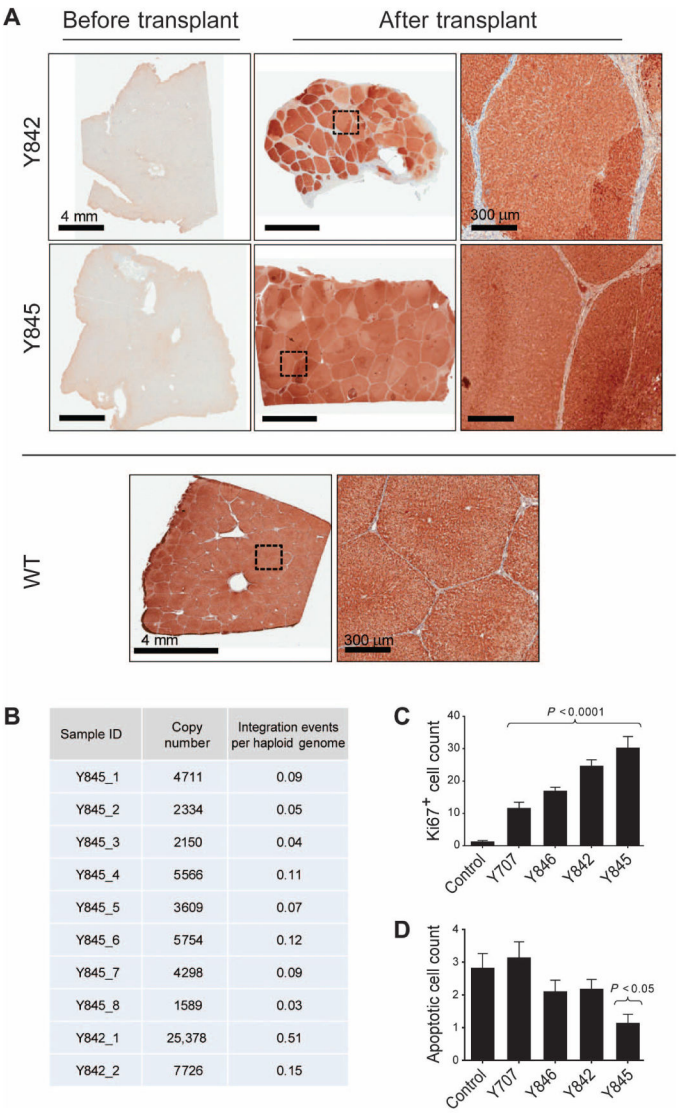

Sample ID	Copy number	Integration events per haploid genome
Y845_1	4711	0.09
Y845_2	2334	0.05
Y845_3	2150	0.04
Y845_4	5566	0.11
Y845_5	3609	0.07
Y845_6	5754	0.12
Y845_7	4298	0.09
Y845_8	1589	0.03
Y842_1	25,378	0.51
Y842_2	7726	0.15

Fig. 5. FAH^{+} hepatocytes completely repopulate the *Fah*$^{-/-}$ liver

(**A**) Representative liver tissues from pigs Y842 and Y845 stained for FAH at the time of hepatectomy (left panels) and 12 months after transplantation with LV-*Fah*–transduced hepatocytes (middle and right panels). An age-matched, nontreated control WT pig is shown for comparison. High-magnification images of the regions outlined by dotted squares are provided. (**B**) DNA from eight different lobes from pig Y845 (1 to 8) and two biopsies from pig Y842 (1 and 2) were analyzed for integration of LV by qPCR. Total copies of integrated LV per 150 ng of genomic DNA were calculated based on a standard curve. The “integration events per haploid genome” were calculated based on the pig haploid genome size of 2800 Mb. (**C**) Ki67-positive nuclei were quantified by counting nuclei in 10 random sections per slide in paraffin-embedded tissue sections of pigs Y707, Y846, Y842, and Y845 and a control WT pig. Data are means ± SEM. *P* values versus control were determined using a two-tailed *t* test. (**D**) Hepatocyte apoptosis was quantified in three random paraffin-embedded tissue sections of pigs Y707, Y846, Y842, and Y845 and a control WT pig.

Apoptotic nuclei were quantified by counting nuclei in 10 random 20× microscopic slides per tissue section. Data are means ± SEM, with statistical significance versus control determined using one-way analysis of variance (ANOVA), followed by Bonferroni's multiple comparisons test.

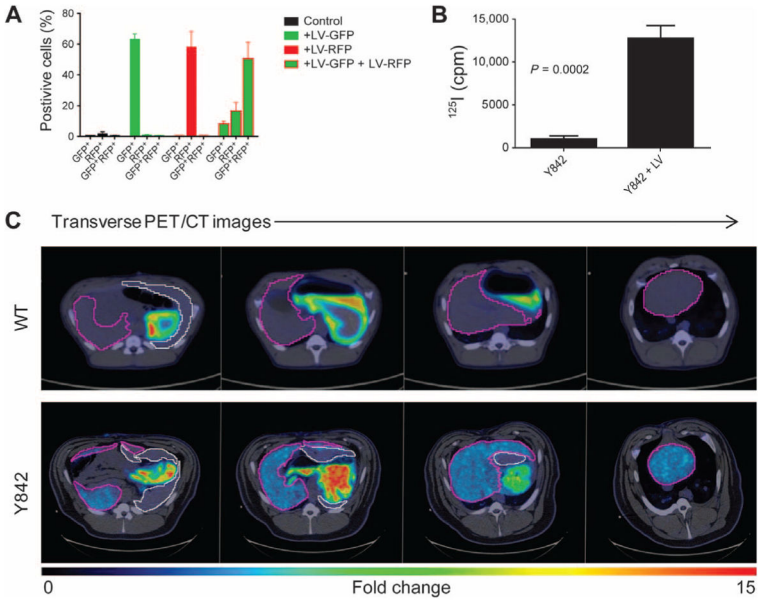

Fig. 6. NIS labeling of cells permits noninvasive detection of repopulating hepatocytes

(**A**) The percentage of GFP^+ and/or RFP^+ hepatocytes after transduction with or without LV-GFP and LV-RFP at an MOI of 500 LPs. Flow cytometry was performed 72 hours after transduction. Data are means ± SD ($n = 3$ replicates). (**B**) In vitro uptake of ^{125}I, measured in counts per minute (cpm), in LV-*Nis*–transduced hepatocytes and control hepatocytes from pig Y842. Data are means ± SD ($n = 3$ replicates). *P* value was determined using a two-tailed *t* test. (**C**) Representative transverse PET/CT images of a control WT pig and pig Y842 after injection of [^{18}F]TFB. Different positions of the liver are shown from head (left side) to feet (right side) of the animals. The relative intensity of [^{18}F] TFB uptake is represented by low (blue) to high (red). The liver is outlined in purple, and the spleen is outlined in white.

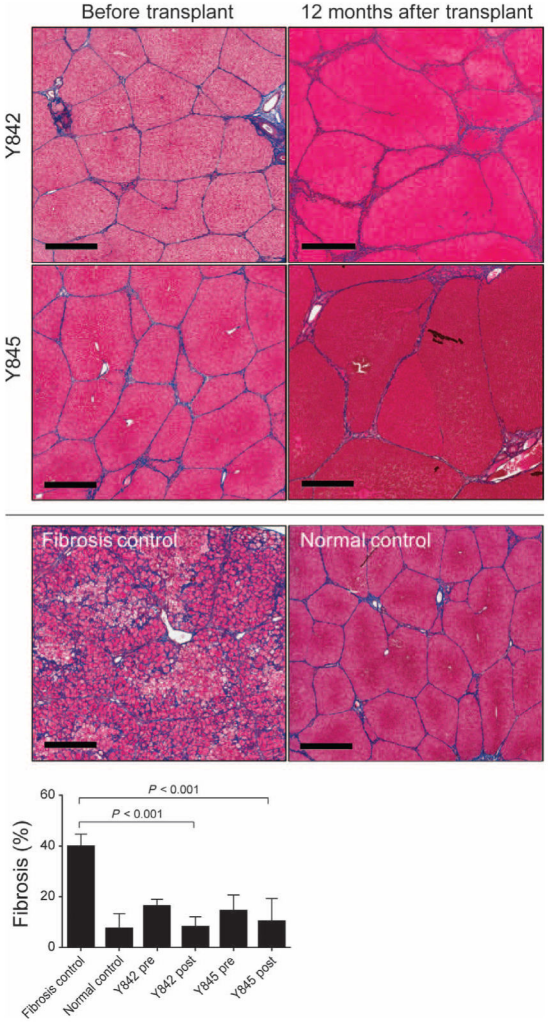

Fig. 7. Ex vivo gene therapy prevents onset of severe fibrosis in *Fah*$^{-/-}$pigs

Representative Masson's trichrome–stained liver sections from pigs Y842 and Y845 are shown at the time of hepatectomy (before transplant) and 12 months after transplantation. A control fibrotic liver from a *Fah*$^{-/-}$pig (14) and WT control are included for comparison. Scale bars, 700 μm. Fibrosis (collagen) in pigs Y842 and Y845 before transplantation (pre) and 12 months after transplantation (post) was quantified and compared to untreated *Fah*$^{-/-}$ animals with fibrosis ($n = 3$) and normal WT ($n = 3$) controls [data for controls are from Hickey *et al.* (12) and Mao *et al.* (14)]. Data are means ± SD. *P* values were determined using a two-tailed *t* test.